Available online at www.scholarsresearchlibrary.com

Scholars Research Library

Archives of Applied Science Research, 2012, 4 (2):914-922
(http://scholarsresearchlibrary.com/archive.html)

ISSN 0975-508X
CODEN (USA) AASRC9

Precision comparison of different monitor unit algorithms using an in-house designed phantom

[1]Aweda MA, [1]Akpochafor MO, [2]Moalosi TGC, [2]Mohlapholi MS and [2]Louw M

[1]College of Medicine, Lagos University Teaching Hospital, Lagos, Nigeria
[2]Tygerberg Academic Hospital, Tygerberge, Cape Town, South Africa

---

ABSTRACT

A phantom for use in radiotherapy treatment planning of human pelvic anatomical region has been designed with six hollows for inserting materials mimicking different biological tissues and the ionization chamber. The yellow plaster of Paris was used to mimic the bone, Styrofoam for the lung and water for soft tissue. The phantom was scanned with Toshiba-Asteion CT-scanner and the images were transferred to the CMS-XiO Treatment Planning System with 3 different algorithms. Measurements of Monitor Units were conducted using 6 MeV photon beams from the ELEKTA-Precise clinical linear accelerator with iso-centric set up. The test of the phantom was done using Fast Superposition (FSS), the Superposition (S) and the Convolution (C) algorithms. Results with FSS algorithm showed better accuracy than S and C. The standard deviation of measurements with bone heterogeneity for all plans varied between +2% and -3%. FSS has faster computation speed than other algorithms; however C has a good balance of speed versus precision in homogeneous medium. Choice of algorithm for use should not be based on the speed of computation alone but also on the accuracy, especially for applications with modern radiotherapy techniques such as intensity modulated radiation therapy (IMRT).

Key words: Phantom, Treatment Planning System, Fast Superposition, Superposition and Convolution Algorithms.

INTRODUCTION

During the management of cancer diseases by radiotherapy, the prescribed radiation dose delivered should be concentrated on the target volume while the doses to normal tissues and organs at risk are minimized. According to Peter Nette and Hans Svensson and other reports in the literature [1-5], a quality assurance program should ensure that all patients treated with a curative aim receive the prescribed dose within a margin of about ±5%. Quality assurance program ensures that all the components of the treatment facilities used in radiotherapy are properly checked for accuracy and consistency and that all radiation generating facilities are functioning according to manufacturer's specification. Following the acceptance and commissioning tests of a computerized TPS, a quality assurance program should be established to verify the performance of the system. Several ways of carrying out the quality assurance of TPS has been proposed by various authors [6-11]. However, it is necessary that each Department develop its own program based on the availability of relevant equipment and according to local requirements, while using standard methods as guideline. Computerized TPS are used in external beam radiotherapy to simulate beam shapes and dose distribution with the intent to maximize tumor control and minimize normal complications [12]. Treatment simulations are used to plan the geometric and radiological aspects of the treatment using radiation transport and optimization principles. TPS facilitate prescribed dose delivery in which a number of parameters of the patient and of the tumor have to be taken into consideration such as the shape, size, depth etc.

There are several algorithms in treatment planning systems that play different roles, however the dose calculation algorithms play the central role of calculating dose distribution within the target volume at any given point [6].

Algorithms are a sequence of instructions that operate on a set of input patient and dosimetric data, transforming the information into a set of desired output results [13]. For every algorithm, the precision of the dose calculation depends on the input parameters used. There are 3 major types of dose calculation algorithms in the CMS Xio TPS for calculating the monitor unit (MU) at a given point with photon beams. These are the Fast Superposition (FSS), the Superposition (S) and the Convolution (C) algorithms, the distribution of dose is convoluted from the total kinetic energy released in material (KERMA) [14]. The FSS algorithm increases the speed of calculation by calculating the radiation dose in the frequency domain [15], while assuming kernels to be invariant with position. Fast Fourier Transform (FFT) convolution does not account for presence of inhomogeneity during calculations and this may lead to inaccurate calculations [13, 16, 17]. Equation 1 describes the dose distribution [18]:

$$D(\vec{r}) = \int \frac{\mu}{p} \psi_p(\vec{r}\,') A(\vec{r} - \vec{r}\,') d^3\vec{r}\,'$$
$$= \int T_p(\vec{r}\,') A(\vec{r} - \vec{r}\,') d^3\vec{r}\,' \quad \text{.................................(1)}$$

$D(\vec{r})$ = dose at a point

μ / p = mass attenuation coefficient

$\Psi_p(\vec{r}\,')$ = primary photon energy fluence

$A(\vec{r} - \vec{r}\,')$ = convolution kernel, the distribution of fraction energy Imparted per unit volume.

$T_p(\vec{r}\,')$ = KERMA at depth includes the energy retained by the photon.

Superposition method employs adaptation of the "collapsed cone" radiation dose calculation method [18, 20]. Energy deposition kernels is modified to account for variations in electron density which makes it suitable for calculating dose in homogenous media compared to FFT convolution Calculation speed is however slow. Equation 2 is used in the Superposition dose calculation [18]:

$$D(\vec{r}) = \int T(\vec{r}\,') \frac{p(\vec{r}\,')}{\bar{p}} K_p(\bar{p}\left|\vec{r} - \vec{r}\,'\right|, \vec{r} - \vec{r}\,') d^3 r' \quad \text{...(2)}$$

where the dose at point $\vec{r}$ is the summation of the KERMA point $T(\vec{r}\,')$ times the value of the energy deposition kernel $H(\vec{r} - \vec{r}\,')$ originating at point r'.

With FSS, the spherical kernels computation is improved by the ability to merge adjacent zenith rays in the kernel [13]. This increases the speed of calculations of the algorithm; however the accuracy of the calculated MU is reduced compared to S algorithm. Depending on the user’s interest, a compromise between the accuracy and speed of calculation is required. Each algorithm surfers some limitations such as the density of the material, due to radiation interactions and the radiation dose deposition points being not modelled, photon and electron contaminations from certain treatment aids not being modeled, the spectrum which is assumed to be independent of the field size and shape, the mass attenuation coefficient, which is used in patient treatment simulation is that of water, electron contamination is assumed to be independent of source to patient skin distance (SSD) and wedge/block trays which are not modeled in the energy fluence calculation. As a result of these limitations it is important to check the accuracy of the algorithms independently. This study aimed at evaluating the precision of the MUs obtained with the algorithms used in CMS XiO TPS using the in-house designed phantom.

MATERIALS AND METHODS

The in-house designed phantom was made in the shape of the human pelvic region. The design was motivated by difficulty in using the Rando Anderson phantom with the diode system for the treatment planning verification measurements. The phantom has provision for six hollow inserts for materials mimicking different biological tissues and the ionization chamber. The yellow plaster of Paris insert (with CT-number = 1100) was used to mimic the bone, Styrofoam (CT-number = - 900) for the lung and water for normal soft tissue. Figures 1 and 2 show the phantom designed with the bone, the lung inhomogeneities and the ionization chamber in position.

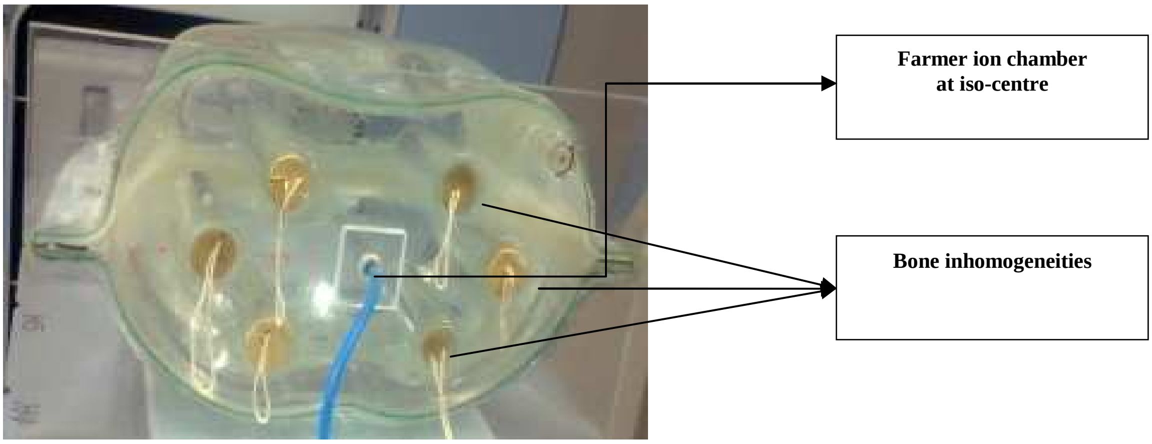

Figure 1: In-house designed phantom filled with water and bone inhomogeneity made of yellow Plaster of Paris (CT-number = 1100)

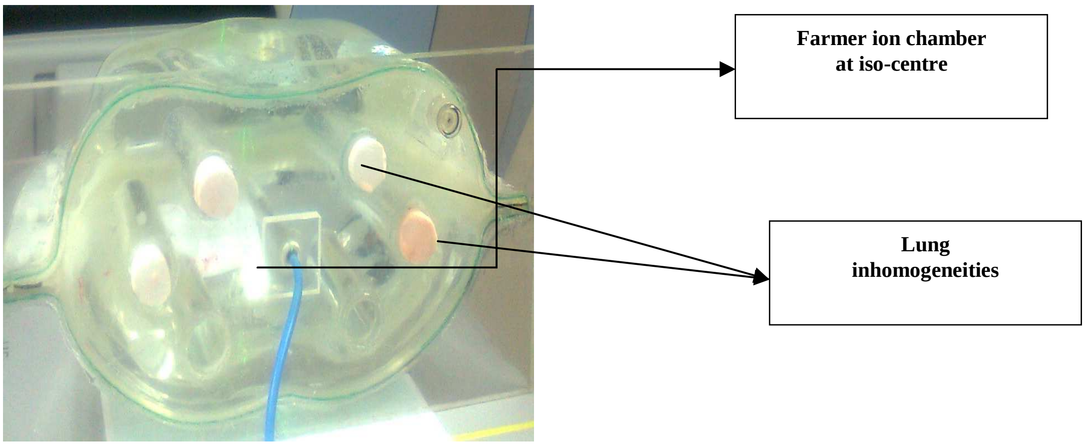

Figure 2: In-house designed phantom with Lung inhomogeneity using Styrofoam (CT number = - 900)

The Toshiba-Asteion CT-scanner was used to acquire images using 5 mm slice thickness. 2 sets of scans were acquired; first with the bone inserts and then lung. From the acquired CT images, the CT-numbers of the bone and lung inhomogeneities were determined using the CT-number calculation algorithm in the CT-scanner. The scanned images were transferred to the CMS-XiO Treatment Planning System for planning as shown in figure 3.

Several simple treatment plans of single and multiple beams were made with the designed phantom using different calculation algorithms configured to give 1.0 Gy at the iso-centre with a 10 x 10 cm² field size, with the set-up as shown in figure 4. The optimal plans were then used with the pre-calibrated ELEKTA-Precise clinical linear accelerator for measurements.

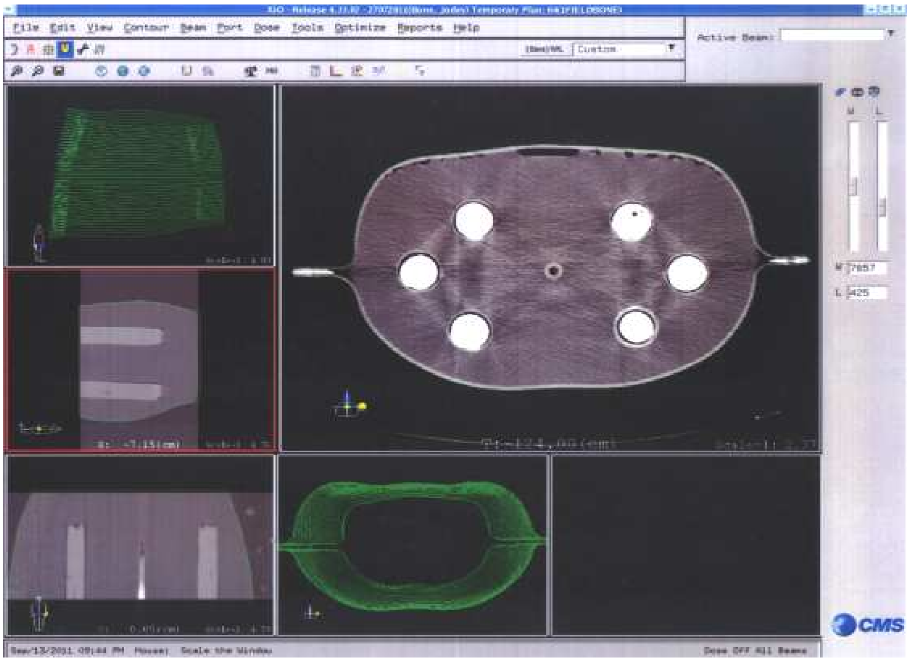

Figure 3: The scans transferred to the CMS-XiO Treatment Planning System for planning

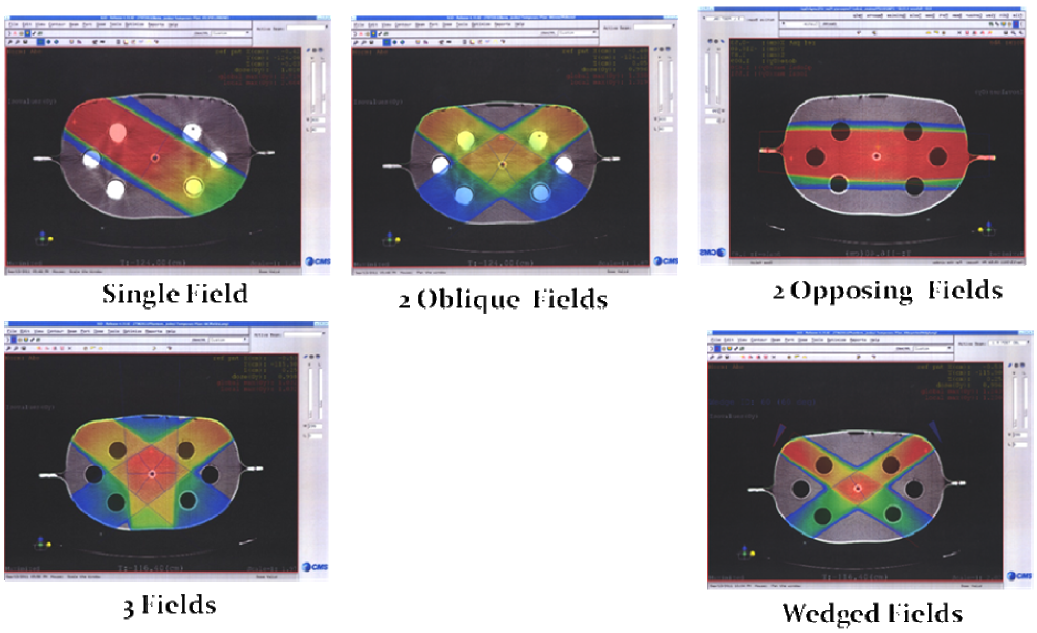

Figure 4: Simple Iso-Centric Plans with 10 x 10 cm2 Field Size

Measurements were conducted using 6 MeV photon beams from the ELEKTA-Precise clinical linear accelerator with iso-centric set up. A pre-calibrated farmer-type ionization chamber along with its electrometer was used to determine the absorbed dose. Necessary corrections for temperature, pressure, polarization, recombination etc were effected on the ionization chamber response. Six measurements were made for each plan using the different algorithms for the purpose of comparison and to limit statistical uncertainties. Absorbed dose at reference depth was calculated as follows [21]:

$$D_{w,Q} = M_Q \times N_{D,w,} \times k_{Q,Qo} \qquad \ldots\ldots\ldots\ldots\ldots\ldots (3)$$

where M_Q is the electrometer reading (charge) corrected for temperature and pressure. $N_{D,w}$ is the chamber calibration factor and $k_{Q,Qo}$ is the factor which corrects for difference in the response of the dosimeter at the calibration quality Q, and at quality Q_o of the clinical x-ray beam according to the TRS 398 protocol of the IAEA. Deviation between expected and measured dose was obtained using equation 4:

$$\% \text{ Deviation} = \frac{D_{meas} - D_{ref}}{D_{ref}} \times 100 \qquad \text{(4)}$$

RESULTS

Tables 1(a-e) show the results of the absorbed radiation doses measured for different photon beams with the bone inhomogeneity, the percentage deviation from the reference dose (1.0 Gy) and the standard deviation for the 6 measurements taken. In tables 1a and 1c, the results with FSS algorithm showed better accuracy compared to others while the Convolution showed lower accuracy. FSS and S showed better accuracy in tables 1b and 1e, however the accuracy of the Convolution improved in table 1d for the 2 opposed field plans. The standard deviation of measurements with bone heterogeneity, for all plans varied within ±4%.

Tables 2(a-e) show the results of the absorbed dose measured with the lung inhomogeneity in position along with the percentage deviation from the reference dose (1.0 Gy) and the standard deviation between the 6 measurements taken. FSS shows better accuracy in tables 2(a-c) compared to C and S. However, the accuracy of C and S on tables 2d and 2e for the opposing fields and 3 field plans improved. The standard deviation of measurements with bone heterogeneity, for all plans varied between +2% and -3%.

Table 1: Measured absorbed dose with bone inhomogeneity for different field plans and percentage deviation from reference dose

(a)

	BONE		
	SINGLE FIELD		
	C	**FSS**	**S**
	1.04	1.02	1.02
	1.04	1.02	1.02
	1.04	1.01	1.02
	1.04	1.01	1.02
	1.03	1.01	1.02
	1.04	1.01	1.02
Average	1.04	1.01	1.02
STD	0.004	0.005	0.001
% Dev	4	1	2

(b)

	BONE		
	WEDGE FIELDS		
	C	**FSS**	**S**
	1.04	1.02	1.03
	1.04	1.03	1.03
	1.04	1.03	1.03
	1.04	1.03	1.03
	1.04	1.03	1.03
	1.04	1.03	1.03
Average	1.04	1.03	1.03
STD	0.001	0.004	0.001
% Dev	4	3	3

(c)

	BONE		
	OBLIQUE FIELDS		
	C	FSS	S
	1.03	1	1.01
	1.03	0.99	1.01
	1.04	1.01	1.02
	1.04	1.01	1.02
	1.04	1.01	1.02
	1.03	1.01	1.02
Average	1.03	1.01	1.02
STD	0.005	0.008	0.005
% Dev	3	1	2

(d)

	BONE		
	2 OPP Fields		
	C	FSS	S
	0.97	0.95	0.95
	0.99	0.97	0.97
	0.98	0.96	0.97
	0.98	0.96	0.97
	0.98	0.96	0.97
	0.98	0.96	0.97
Average	0.98	0.96	0.97
STD	0.006	0.006	0.008
% Dev	-2	-4	-3

(e)

	BONE		
	Three Fields		
	C	**FSS**	**S**
	1.03	1.00	1.01
	1.03	1.01	1.01
	1.03	1.01	1.02
	1.03	1.01	1.01
	1.02	1.01	1.01
	1.02	1	1.02
Average	1.03	1.01	1.01
STD	0.006	0.005	0.005
% Dev	3	1	1

Table 2: Measured absorbed dose with lung inhomogeneity for different field plans along with the percentage deviation from the reference dose

(a)

	LUNG		
	SINGLE FIELD		
	C	**FSS**	**S**
	1.03	1.02	1.03
	1.02	1.01	1.02
	1.02	1.01	1.02
	1.02	1.01	1.02
	1.02	1.01	1.02
	1.02	1.01	1.02
Average	1.02	1.01	1.02
STD	0.004	0.004	0.004
% Dev	2	1	2

(b)

	LUNG		
	WEDGE FIELDS		
	C	**FSS**	**S**
	1.02	1.02	1.02
	1.02	1.01	1.02
	1.02	1.01	1.02
	1.02	1.01	1.02
	1.02	1.01	1.02
	1.02	1.01	1.02
Average	1.02	1.01	1.02
STD	0.001	0.004	0.001
% Dev	2	1	2

(c)

	LUNG		
	OBLIQUE FIELDS		
	C	**FSS**	**S**
	1.03	1.01	1.03
	1.02	1.02	1.02
	1.02	1.01	1.02
	1.02	1.01	1.02
	1.02	1.01	1.02
	1.02	1.01	1.02
Average	1.02	1.01	1.02
STD	0.004	0.004	0.004
% Dev	2	1	2

(d)

	LUNG		
	OPPOSING FIELDS		
	C	**FSS**	**S**
	0.98	0.97	0.97
	0.97	0.96	0.97
	0.97	0.97	0.97
	0.97	0.97	0.97
	0.97	0.97	0.97
	0.97	0.97	0.98
Average	0.97	0.97	0.97
STD	0.004	0.004	0.004
% Dev	-3	-3	-3

(e)

	LUNG		
	THREE FIELDS		
	C	**FSS**	**S**
	1.02	1.01	1.01
	1.02	1.01	1.01
	1.01	0.99	1.00
	1.01	0.99	1.00
	1.01	0.99	1.01
	1.01	1.00	1.01
Average	1.01	0.99	1.01
STD	0.005	0.009	0.005
% Dev	1	-1	1

Tables 3(a-e) show the results of the absorbed dose measured in solid water along with the percentage deviation from the reference dose (1.0 Gy) and the standard deviation between the 6 measurements taken. C and S showed better accuracy in tables 3a and 3c. FSS was better in table 3b for the wedged fields and S better in table 3d for the opposed fields. FSS and S showed improved accuracy for the 3 field plans in table 3e. The standard deviation of measurements with bone heterogeneity, for all plans varied between +3% and -2%.

Table 3: Measured absorbed dose solid water for different field plans along with the percentage deviation from the reference dose

(a)

	SOLID WATER		
	SINGLE FIELD		
	C	**FSS**	**S**
	1.01	1.03	1.01
	1.00	1.02	1.01
	1.01	1.02	1.00
	1.01	1.02	1.01
	1.00	1.02	1.01
	1.01	1.03	1.02
Average	1.01	1.02	1.01
STD	0.005	0.005	0.006
% Dev	1	2	1

(b)

	SOLID WATER		
	WEDGE FIELDS		
	C	**FSS**	**S**
	1.03	1.03	1.03
	1.04	1.02	1.03
	1.03	1.03	1.03
	1.03	1.03	1.03
	1.03	1.02	1.03
	1.03	1.02	1.02
Average	1.03	1.02	1.03
STD	0.004	0.006	0.004
% Dev	3	2	3

(c)

	SOLID WATER		
	OBLIQUE FIELDS		
	C	**FSS**	**S**
	1.01	1.02	1.01
	1.02	1.01	1.02
	1.01	1.02	1.01
	1.01	1.02	1.01
	1.01	1.02	1.01
	1.01	1.01	1.02
Average	1.01	1.02	1.01
STD	0.004	0.005	0.005
% Dev	1	2	1

(d)

	SOLID WATER		
	OPPOSING FIELDS		
	C	**FSS**	**S**
	1.00	0.98	1.00
	0.99	0.99	0.99
	0.98	0.98	1.00
	1.00	0.98	1.00
	0.99	0.98	0.99
	1.00	0.98	1.00
Average	0.99	0.98	1.00
STD	0.006	0.004	0.005
% Dev	-0.1	-2	0

(e)

	SOLID WATER		
	THREE FIELDS		
	C	**FSS**	**S**
	1.03	1.02	1.02
	1.02	1.02	1.02
	1.03	1.01	1.00
	1.03	1.00	1.01
	1.02	1.02	1.01
	1.02	1.00	1.01
Average	1.02	1.01	1.01
STD	0.005	0.009	0.008
% Dev	2	-1	1

DISCUSSION AND CONCLUSION

The variations in the results of the treatment plans comparing the 3 algorithms using the designed phantom were within the ±4% limit proposed by van Dyk et al. in 1993 [6] and they follow a trend similar to those of Butts and Foster [17], who used Anthropomorphic phantom. Wider variations observed with the Convolution algorithm at the bone inhomogeneity could be adduced to the scattered radiation unaccounted for in the inhomogeneous material [13, 22]. Convolution appeared good where there are no inhomogeneities as could be seen in table 3. There is a general improvement in the results for all algorithms in the 3 field plans while small deviation is noticeable for the wedged field plans across board. This may likely be due to the inability of the algorithms to model the energy fluence calculation for wedges [6, 7]. There is a similar trend observed in the results of the FSS and S, this is due to the similarity in the methods (collapse cone) which both algorithms used for calculations. FSS has a faster computation speed compared to other algorithms, however convolution has a good balance of speed versus precision in homogeneous medium. The possibility of the combination of the convolution and the superposition to yield better outcome has been discussed in some reports [23 - 28]. With such combination, dose can be more accurately computed at a single point in both homogeneous and inhomogeneous media with increase in speed compared to the normal FFT convolution. Other sources of uncertainty such as set-up, phantom and the detector could have as well contributed to deviations.

The choice of which algorithm to use should not be based on the speed of computation alone but also on the accuracy, especially for applications with modern radiotherapy techniques such as intensity modulated radiation therapy (IMRT), where high accuracy of delivered dose is required. Hence, the goal would be to strike a balance between speed and accuracy. Each algorithm has its advantages and shortfalls based on the assumptions made during the design. However, our results from tables 1 and 2 show that all the 3 algorithms may be used successfully for the calculation of the MU to an accuracy of ±4%. There is no significant difference in the results obtained in tables 1 and 2 with the designed phantom and those in table 3 with solid water phantom. This shows that the materials used in the design of the in-house phantom, used for testing the 3 algorithms were suitable and that the phantom can be used successfully for routine verification exercises. Also, the cost of designing the phantom is minimal and it is easier to use compared to other modern phantoms like the Rando Anderson phantom. Radiotherapy centers without diode or TLD systems available can conduct verification exercises using this phantom with local ionization chamber.

REFERENCES

[1]. P. Nette, H. Svensson. Radiation dosimetry in health care; expanding the reach of global networks. Viena: IAEA bulletin. **April 1994**.
[2]. ICRU Reports 24. Determination of absorbed dose in a patient irradiated by beams of X or gamma rays in radiotherapy procedures. Washington DC: ICRU publication. **1976**.
[3]. A. Brahme. *Acta Radiol. Oncol*. **1984**, 23, 379-391.
[4]. A. Brahme. *Radiother. Oncol*. **1988**, 12, 129-140.
[5]. BJ. Mijnheer, JJ. Battermann, A. Wambersie. *Radiother. Oncol*. **1987**, 8, 237-252.
[6]. EB Podgorsak. Radiation Oncology Physics: A handbook for Teachers and Students. Vienna: IAEA publication. **2005**.
[7]. J. Van Dyk, RB. Barnett, JE. Cygler, PC. Shragge. *Int. J. Radiat. Oncol. Biol. Phys.* **1993**, 26,261–273.

[8]. J. Van Dyk. "Quality Assurance." In Treatment Planning in Radiation Oncology. Khan FM, Potish RA (Eds.). (Baltimore, MD: Williams and Wilkins). **1997**, 123–146.
[9]. JE. Shaw. (Ed.) "A Guide to Commissioning and Quality Control of Treatment Planning Systems." The Institution of Physics and Engineering in Medicine and Biology. **1994**.
[10]. BA. Fraass, K. Doppke, M. Hunt, G. Kutcher, G. Starkschall, R. Stern, J. Van Dyk. *Med. Phys.* **1998**, 25, 1773–1829.
[11]. BA. Fraass. "Quality Assurance for 3-D Treatment Planning." In Teletherapy: Present and Future. Palta J, Mackie TR (Eds.). Madison: Advanced Medical Publishing. **1996**, 253–318.
[12]. TR. Mackie, JW. Scrimger, JJ. Battista. *Med Phys.* **1985**, 12, 188–96.
[13]. AL. Boyer, Y. Zhu, L. Wang, P. Francois. *Med. Phys*. **1989**, 16, 248–253 .
[14]. Animesh. *J Cancer Res Ther*. **2005**, 1, 12-20.
[15]. A. Ahnesjo. *Med. Phy.* **1989**, 16, 577-592.
[16]. MM. Miften, AW. Beavis, LB. Marks. *Med Dosim*. **2002**, 27, 51–57.
[17]. IAEA Technical Report Series 398. Absorbed dose determination in external beam radiotherapy: an international code of practice for dosimetry based on standards of absorbed dose to water. Vienna: IAEA publication. **2000**, 1011-4289.
[18]. KR. Muralidhar, NP. Murthy, AK. Raju, N. Sresty, *J Med Phys* **2009**, 34, 12-22 .
[19]. TR. Mackie, A. Ahnesjo, P. Dickof, A. Snider. "Development of a convolution/superposition method for photon beams," Use of Comp. In Rad. Ther.**1987**, 107-110.
[20]. TR. Mackie, PJ. Reckwerdt, TW. Holmes, SS. Kubsad. "Review of convolution/superposition methods for photon beam dose computation," Proceedings of the Xth ICCR.**1990**, 20-23.
[21]. TR. Mackie, PJ. Reckwerdt, MA. Gehring, TW. Holmes, SS. Kubsad, BR. Thomadsen, CA. Sanders, BR. Paliwal, TJ. Kinsella. "Clinical implementation of the convolution/superposition method," Proceedings of the Xth ICCR. **1990,** 322-325.
[22]. F. Hasenbalg, H. Neuensch wander, R. Mini, EB. Born. *J. Phy. Conf. Ser*. **2007**.
[23]. B. Vanderstraeten, N. Reynaert, L. Paelinck, I. Madani, C. De Wagter, W. De Gersem. *Med. Phys* **2006**, 33, 3149.
[24]. E. Born, A. Fogliata-Cozzi, F. Ionescu, V. Ionescu, PA. Tercier. *Swiss Soc. Radio. Med. Phy*. **1999**.
[25]. JR. Butts, AE. Foster. *J. App. Clin. Med. Phy*. **2001**, 2, 1526-9914.
[26]. TR. Mackie, E. El-Kathib, J. Battista, JW. Scrimger, J. Van Dyk, JR. Cunningham. *Med Phys* **1985**, 12, 327-32.
[27]. **R.** Kohno, S. Kitou, E. Hirano, S. Kameoka, T. Goka, T. Nishio et al. *Radiol. Phy. Tech*. **2009**, 2, 87-96.